Published in final edited form as:

Curr Biol. 2022 August 22; 32(16): 3545–3555.e4. doi:10.1016/j.cub.2022.06.069.

A promoter-proximal silencer modifies the activity of a shared enhancer to mediate divergent expression of *nub* and *pdm2* paralogs in wing development

Ryan Loker[1], **Richard S. Mann**[1,2]

[1]Department of Biochemistry and Molecular Biophysics, Columbia University

[2]Department of Neuroscience, Department of Systems Biology, Mortimer B. Zuckerman Mind Brain Behavior Institute, Columbia University

Summary

Duplication of genes and their associated *cis*-regulatory elements, or enhancers, is a key contributor to genome evolution and biological complexity. Moreover, many paralogs, particularly tandem duplicates, are fixed for long periods of time under the control of shared enhancers. However, in most cases the mechanism by which gene expression and function diverge following duplication is not known. Here we dissect the regulation and function of the paralogous *nubbin*/*pdm2* genes during wing development in *Drosophila melanogaster*. We show that these paralogs play a redundant role in the wing and that their expression relies on a single shared wing enhancer. However, the two genes differ in their ability to respond to this enhancer, with *nub* responding in all wing progenitor cells and *pdm2* only in a small subset. This divergence is a result of a *pdm2*-specific silencer element at the *pdm2* promoter that receives repressive input from the transcription factor Rotund. Repression through this silencer also depends on *nub*, allowing *pdm2* to fully respond to the wing enhancer when *nub* expression is perturbed and functional compensation to occur. Thus, expression divergence downstream of a shared enhancer arises as a consequence of silencing the promoter of one paralog.

eTOC blurb

Loker and Mann show that two closely related paralogs in *Drosophila*, *nub* and *pdm2*, function redundantly in wing development and, although they are regulated by the same enhancer in wing discs, they have distinct expression patterns due to wing disc-specific repression of *pdm2* through its promoter.

*Correspondence and Lead Contact: Richard S. Mann; rsm10@columbia.edu.

Author Contributions: R.L: Conceptualization, Methodology, Investigation, Formal analysis, Visualization, Writing – Original Draft, Writing – Review&Editing. R.S.M: Conceptualization, Methodology, Writing – Original Draft, Writing – Review&Editing, Funding acquisition

Twitter: @richmann10

Declaration of interests: The authors have no competing interests to declare

Graphical Abstract

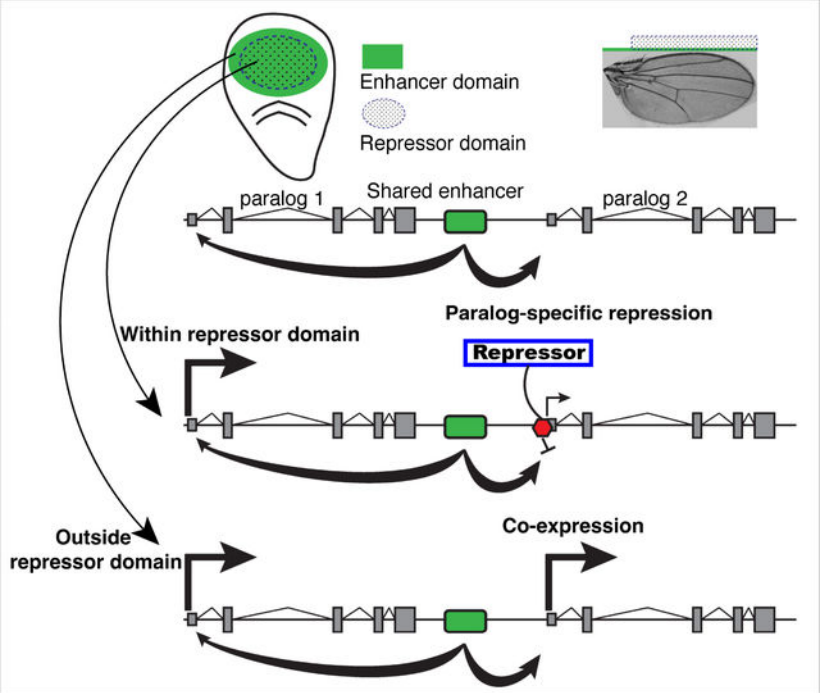

Introduction

A major driver of genome evolution and biological diversity is the acquisition of new genes via duplication [1]. As such, the mechanisms by which duplicated genes are retained in the genome and their potential evolutionary trajectories are of great interest. While the majority of genes resulting from duplication events are quickly lost through a process known as nonfunctionalization [2], preservation of paralogs in the genome is thought to occur via a number of mechanisms [3,4]. Duplicated genes can diverge either by acquiring new functions (neofunctionalization [1]) or by the partitioning of ancestral functions, as originally described by the Duplication-Degeneration-Complementation (DDC) or subfunctionalization models [2]). However, preserved duplicates can also persist without an observable divergence in expression or function, where they may maintain functional redundancy over long periods of time [5,6]. Redundancy due to gene duplication has also been proposed to aid in robustness of biological processes in response to environmental or genetic perturbations [7,8]. In all eukaryotes that have been studied, a particularly strong propensity for co-expression is found for paralogs that exist close to one another in the genome, called tandem duplicates [6,9,10]. One explanation that has been proposed for the high prevalence of co-expression for tandem duplicates is that they may be under control of a shared set of *cis*-regulatory elements or enhancers. Co-dependence on a single regulatory element would also explain why some tandem duplicates have conserved synteny over long evolutionary time scales. However, the functional validation of shared enhancers has only been demonstrated in a small number of instances [6,11]. Moreover, because of their dependency on the same enhancers, it is less clear how tandem duplicates can evolve complementary or novel functions.

Here we present an analysis of the expression and function of the paralogous *nubbin* (*nub*, also known as *pdm1*) and *pdm2* genes during development of the wing appendage in *Drosophila melanogaster*. *nub* and *pdm2* arose in an ancient duplication near the base of the divergence of the Brachycera suborder around 200 million years ago (Figure 1A). Both genes encode similar POU-type homeodomain transcription factors (TFs) (Figure S1A) and play a role in development of a wide variety of cell types [12–15] In winged insects (Pterygota) *nub* is a conserved marker for wings and has been shown to be essential for wing development from beetles to flies [12,14,16,17]. *nub* is expressed throughout the wing primordia in the *Drosophila* wing imaginal disc, including the progenitors of both the distal hinge and wing blade. Strong wing phenotypes are observed in multiple alleles attributed to loss of *nub* expression [12,14]. We show, however, that *nub* is dispensable for wing development in *Drosophila* as a result of compensation by *pdm2*, revealing a previously unknown redundancy of these paralogs during wing development. Further, the wing phenotype of a classical *nub* allele is a result of a deletion of a shared wing enhancer that is essential for both *nub* and *pdm2* expression in wing progenitor cells. Surprisingly, although the expression of both genes in the wing depend on the same enhancer, the expression patterns of *nub* and *pdm2* differ under normal developmental conditions. The cause of this divergent expression is a *pdm2*-specific silencer element localized to its promoter (~20 kb from the enhancer) that blocks the response to the shared enhancer in most wing cells. Repression through this element requires direct input from the TF Rotund (Rn). *nub* is also required for *pdm2* repression and, in the absence of *nub*, *pdm2* responds to the shared enhancer in all wing cells, revealing the mechanism for its compensatory function. Altogether this study highlights a case in which redundant paralogs that depend on the same enhancer have divergent expression patterns because of repressive inputs into one of their promoters, thus revealing a novel mechanism for how tandem duplicates can evolve distinct functions.

Results

Functional redundancy of nub *and* pdm2 *in wing development*

Classical regulatory alleles of *nub* cause severe growth and tissue organization defects of the adult wing [12,14]. Surprisingly, however, when Nubbin protein is specifically depleted during wing development, either through RNAi knockdown [18] or somatic CRISPR targeting of the gene locus (Figure 1B), the wings appear normal. To examine if the lack of wing phenotype could be due to a redundant function of the paralogous *pdm2* gene, we repeated the somatic CRISPR loss-of-function experiments in the background of the $pdm2^{E46}$ allele, which produces a truncated protein as a result of a premature termination codon prior to the homeodomain [15]. Animals lacking *pdm2* are viable and have morphologically normal wings (Figure 1C). Furthermore, wing imaginal discs from $pdm2^{E46}$ larvae lack staining by Pdm2-specific antibody (Figure S1B). When *nub* is mosaically removed in wings that also lack *pdm2* the adult appendage shows defects similar to wings containing clones of cells with classical *nub* regulatory alleles, characterized by reduction of hinge organization, overall wing size, and ectopic margin bristles in the interior blade region (Figure 1D–E, [12,14]. The mosaic phenotype in this background is a result of incomplete knockout from the CRISPR targeting, which can be visualized from clonal loss of Nub protein in the wing disc and confirms the efficacy of the CRISPR-mediated knockout (Figure S1C). These

observations imply that 1) *pdm2* and *nub* can function redundantly during wing development and 2) that classic loss of function *nub* alleles disrupt the expression of both *nub* and *pdm2*. Below, we test and confirm both of these predictions.

Compensation of nub *loss-of-function by upregulation of* pdm2

We next examined the expression of Nub and Pdm2 within wing progenitor tissue during development. Although Nub expression levels appear uniform throughout the appendage-generating domain of the wing imaginal disc, Pdm2 expression is limited to a subset of progenitor cells at the periphery of the appendage domain that express high levels, while more distal cells have weak or no detectable protein (Figure 2A–B). Notably, the anti-Nubbin antibody used here and previously [16] recognizes both Nub and Pdm2 proteins while the anti-Pdm2 antibody specifically labels Pdm2 (data not shown). Given that Pdm2 is only appreciably expressed in the outer edge of the distal hinge domain, we conclude that anti-Nub staining in the central appendage domain is largely the result of Nub protein only, whereas in the edge of the distal hinge the signal results from the co-expression of Nub and Pdm2 (Figure 2C). To confirm this, we analyzed the expression of a *nub-GFP* allele, where GFP was knocked-in to the endogenous C-terminal end of the *nub* coding sequence using CRISPR/Cas9 (Figure S2). Nub-GFP protein is expressed throughout the entire wing progenitor domain, including the Pdm2+ cells, thus confirming that *nub* is expressed uniformly in the pouch and distal hinge domains.

The differences in expression between Nub and Pdm2 raise the question of how *pdm2* can compensate for loss of *nub* during wing development. We tested the idea that *pdm2* is upregulated in the absence of *nub*. Consistent with this idea, we find that Pdm2 levels increase throughout the wing pouch domain following loss of *nub* induced by somatic CRISPR (Figure 2D) or upon RNAi induced knockdown specifically in the Posterior compartment using the *engrailed* Gal4 for which comparison with adjacent anterior cells serves as an internal control (Figure 2E).

The nub^{1} *allele is a regulatory mutant that removes both* nub *and* pdm2 *expression*

The results explained thus far demonstrate that both *nub* and *pdm2* are each sufficient for wing development, and therefore raise the question of how previously described *nub* alleles display strong wing phenotypes. Multiple viable alleles of *nub* have been described that develop wing malformations and each is associated with insertions or re-arrangements within non-coding regions near the *nub* locus [14]. We focused on the *nub^{1}* allele, which displays a very strong wing phenotype (Figure 1E) [12,14]. We first performed RNA-seq using wing discs from *nub^{1}* animals and compared the *nub* and *pdm2* transcript levels with wild type tissue. This analysis showed that *nub* levels were drastically reduced and *pdm2* transcripts were undetectable in the *nub^{1}* background (Figure 3A). Antibody staining of *nub^{1}* wing discs revealed that most of the tissue lacks Nubbin protein, with only two small clusters of cells retaining some expression, as previously reported [12]. Antibody staining for Pdm2 revealed that it was nearly absent in *nub^{1}* wing discs, consistent with the RNA-seq analysis (Figure 3B). Analysis of mitotic clones with the *nub^{1}* allele reveals that cells in the domain that retain some Nub expression display lower levels of protein compared to wild type cells (Figure S3A). These results suggest that the phenotype associated with the

nub^{1} allele is due to loss of expression of both *nub* and *pdm2* during wing development. To further establish that *nub*-associated wing phenotypes are associated with loss of both paralogs, we examined protein levels in wing discs of a different allele that causes a strong wing phenotype, *nub*^{2} [14]. Consistent with the *nub*^{1} result, *nub*^{2} wing discs show a similar loss of Nub and Pdm2 (Figure S3B). In the next sections we investigate the mechanism by which expression of both genes is impaired in the *nub*^{1} genetic background.

A wing enhancer element is deleted in the nub^{1} *allele*

The *nub*^{1} allele has previously been shown to have an insertion of the 412 transposon into the promoter of one of two *nub* isoforms [14]. However, this insertion is unlikely to explain the loss of expression of both paralogs. As part of our investigation of Nub function in the wing (discussed below) we performed Assay for Transposase Accessible Chromatin with high-throughput sequencing (ATAC-seq) in wild type and *nub*^{1} imaginal discs. ATAC-seq relies on Tn5 transposase insertion and cutting of genomic DNA, which occurs preferentially at open chromatin regions though also to a lower degree in all genomic regions [19]. Surprisingly, this analysis revealed a segment of DNA between *nub* and *pdm2* that had no ATAC-induced sequence reads from homozygous *nub*^{1} wing discs compared to wild type wing discs (Figure 3C). The most likely explanation is that this region is absent in the *nub*^{1} genome. To test this idea we directly sequenced the locus by Sanger sequencing, which confirmed that a sequence of 1,824 base pairs was missing in the *nub*^{1} genome (Figure S3C). Thus *nub*^{1} contains a previously unknown 1.8 kb deletion in the intergenic region between *nub* and *pdm2*.

We next asked if the missing DNA fragment contains transcriptional regulatory activity. Previously, a large scale enhancer screen was performed and non-coding segments within the entirety of the *nub*/*pdm2* genomic locus were assayed for their ability to drive reporter gene expression [20]. One fragment tested, GMR11F02, contains the entirety of the region deleted in the *nub*^{1} allele. When placed within a construct containing the *Drosophila* synthetic core promoter (DSCP) upstream of Gal4 coding sequence, UAS-driven reporter expression is observed throughout the developing wing appendage domain (Figure 3D). Thus a DNA fragment that includes the *nub*^{1} deletion has a previously unknown wing enhancer. Notably, among all cloned segments tiling the 140 kb *nub*/*pdm2* locus, GMR11F02 was the only fragment to drive an expression pattern similar to the *nub* expression domain (Jory et al., 2012). Below, the regulatory element contained within the GMR11F02 region will be referred to as the Nubbin-Pdm2-Wing (NPW) enhancer. In the next section we determine the extent to which NPW enhancer deletion contributes to the *nub*^{1} phenotype and its influence on expression of *nub* and *pdm2*.

A nub/pdm2 shared enhancer is essential for wing development

The previous results show that the *nub*^{1} genotype is associated with a deletion of a wing enhancer contained within the GMR11F02 segment. As this allele also contains a 412 transposon insertion, and could have additional unknown abnormalities within the *nub*/*pdm2* locus, we next determined if the enhancer deletion was sufficient to cause the *nub*^{1} wing phenotype. To do this, we removed the NPW enhancer in an otherwise wild type background using CRISPR/Cas9. Two deletions were made: one corresponding closely to the missing

segment in *nub*^{1} (NPW-small), and another that contains additional DNA present in the GMR11F02 segment (NPW-large) (Figure 4A–B). Flies containing the NPW-small deletion are homozygous viable with a strong wing phenotype similar to that of the *nub*^{1} animals (Figure 4C – compare with Figure 1E). The phenotype of adult flies containing NPW-large is indistinguishable from that of the smaller deletion (Figure 4C), suggesting that the region deleted in *nub*^{1} strain, corresponding to the NPW-small boundaries, removes the entire NPW enhancer. This result confirms that the primary cause of the *nub*^{1} phenotype is the absence of this enhancer element.

Because both *nub* and *pdm2* are sufficient for wing development, we next asked whether expression of both genes is dependent on this enhancer. Indeed, as in the *nub*^{1} background, both Nub and Pdm2 proteins are absent in the majority of the wing disc, with a small number of cells in the central region of the appendage domain retaining low levels of Nub (Figure 4C). Thus, this regulatory region is used by both paralogs during wing development. In distal hinge cells at the periphery of the wing progenitor domain the NPW enhancer is required for activation of both *nub* and *pdm2*. Under normal conditions in the rest of the appendage domain it preferentially activates *nub* due to repression of *pdm2*, but in the absence of *nub*, the NPW enhancer is also required to activate *pdm2*.

Paralog specific response to NPW is due to repression by the Rotund transcription factor

Although Nub is essential for repression of *pdm2* in the central wing domain, additional spatial factors must be required as *pdm2* is not repressed in the *nub*+ cells at the periphery of the appendage domain. We looked for a potential candidate whose expression boundary in the wing disc is defined by where *pdm2* repression occurs. The transcription factor Rotund (Rn) is expressed in the central domain of the wing, encompassing the entire pouch and extending partially into the distal hinge [21]. Co-staining a Rn-GFP allele tagged at the endogenous gene locus [22] and Pdm2 shows that the expression of Pdm2 and Rn is largely mutually exclusive (Figure 5A). To ask if Rn participates in *pdm2* repression, we examined Pdm2 levels in wing discs from flies containing a *rn* null allele. Consistent with a function for *rn* in repression of *pdm2*, we find de-repression of *pdm2* throughout the central wing disc in the absence of *rn* (Figure 5B). RNAi mediated knockdown of *rn* specifically in the posterior compartment driven by *engrailed* also causes derepression of Pdm2 specifically in posterior cells, and the comparison with adjacent anterior cells serves as an internal control (Figure S4A). We next asked whether *rn* expression is dependent on *nub*, as this could potentially mediate the repression of *pdm2* by *nub,* and found that *rn* is expressed normally in the *nub*^{1} background (Figure S4B). Conversely, *nub* expression remains unaffected in the absence of *rn* (Figure 5B). Thus *nub* and *rn* do not regulate each other and are independently required for repression of *pdm2* in the central wing domain under normal conditions.

If *rn* is the limiting factor that defines where *pdm2* is repressed, then ectopic expression of *rn* in the *pdm2*-expressing cells should be sufficient to repress *pdm2*. To test this we generated clones that ectopically express Rn. Expression of Rn in cells that normally express high levels of *pdm2* cause autonomous repression of *pdm2* (Figure 5C). In summary, *rn* is a *pdm2*-specific repressor that causes *nub* and *pdm2* to respond differently to the NPW enhancer.

Rotund directly binds to the Pdm2 promoter

We next sought to identify the mechanism by which *rn* represses *pdm2*. As the NPW enhancer is shared by *nub* and *pdm2,* any repressive input into this regulatory element would likely affect both genes. Thus, we hypothesized that *rn* modifies *pdm2* expression through *cis*-acting regions outside of NPW or that *rn* represses *pdm2* indirectly. To ask if Rn binds to regions within the *nub*/*pdm2* genomic complex we performed Chromatin Immunoprecipitation with Sequencing (ChIP-seq) using the *rn-GFP* allele [22] with chromatin derived from otherwise wild type 3rd instar wing imaginal discs. Analysis of all regions of enriched ChIP-seq signal throughout the genome (i.e ChIP peaks) revealed a high degree of specific enrichment for the canonical Rn binding motif, suggesting that the experiment successfully identified Rn target sites (Figure S5A). Within the ~140 kb *nub*/*pdm2* locus, there is a cluster of Rn peaks at the *pdm2* promoter, and weaker peaks at the promoters of *nub* and *ref2* (which overlaps the gene body of *nub* and is transcribed on the opposite strand) (Figure S5B). Given that our functional data show a specific effect of *rn* on *pdm2* expression, we hypothesized that the *pdm2*-specific response to NPW may be mediated by the cluster of Rn binding events within the *pdm2* promoter region (Figure 6A).

As Nub is also required for repression, we attempted a similar strategy to map its binding in the wing imaginal disc. To do so we utilized the *nub-GFP* knock-in allele described above and performed ChIP-seq on wing disc-derived chromatin. While this analysis revealed enrichment around the *pdm2* promoter, the global analysis failed to meet our criteria for a successful ChIP experiment. Specifically, the Nub motif enrichment in the genome-wide peak set was lower than that of general open-chromatin associated transcription factors such as GAF. Thus, whether Nub directly binds to the *pdm2* promoter remains an open question.

The pdm2 promoter represses NPW activity

To test the hypothesis that the promoter region of *pdm2* is capable of modifying NPW enhancer activity, we utilized an enhancer-reporter system to test the effect of different promoters on NPW-dependent transcription. As discussed previously, GMR11F02, which contains NPW, drives reporter activity in the entire wing domain when placed upstream of a synthetic minimal promoter (Figure 3D and Figure 6E). When the synthetic promoter is replaced with a 444 nucleotide region comprising the putative *pdm2* promoter region, reporter activity recapitulates the pattern of the endogenous *pdm2* gene (Figure 6C). When observed in a *rn* null genetic background, in which *pdm2* expression is derepressed (see Figure 5B), reporter activity is also derepressed in most of the distal hinge and dorsal-ventral (DV) boundary, and to a lesser extent in the pouch cells surrounding the DV boundary (Figure 6D). This result is consistent with the ability of the *pdm2* promoter to modify the regulatory activity downstream of NPW in a Rn-dependent manner. We also observed the same response in the haltere imaginal disc, which is specified by an analogous genetic program as the wing, with an additional input by the *Hox* gene *Ultrabithorax* (*Ubx*) [23,24] (Figure S5C).

Repression of the pdm2 *promoter by Rn is mediated by multiple binding sites*

To identify the Rn binding sites within the *pdm2* promoter that mediate repression we searched for matches to the Rn binding motif and assayed the effect of mutation of

these sites on reporter activity. Because GMR11F02 has the capacity to function in all wing cells, mutation of repressive binding sites within the *pdm2* promoter should restore activity to the pattern observed when the synthetic promoter is used. Two Rn motifs proximal to the transcription start site are located within in a highly conserved block of 27 nucleotides conserved in all *Drosophila* species (referred to as motif #1 and 2, Figure S5D). Furthermore, motif #1 and the surrounding 18 nucleotides are conserved within the distantly related housefly genome. An additional 6 motifs resembling Rn binding sites are present in the *D. melanogaster* genome that vary in their degree of conservation with other *Drosophila* species (Figure 6B and Figure S5D). We generated four reporter variants to test the effect of these binding sites on NPW repression: 1) conserved motif #1 mutated, 2) conserved motif #2 mutated, 3) conserved motif #1+#2 mutated, and 4) all eight motifs mutated. Mutation of the motifs contained with the larger conservation block individually each results in expanded expression within the *rn*+ domain to varying degrees. Mutation of conserved motif #1 causes slight expansion of reporter activity distally in the hinge and derepression along the DV boundary (Figure 6G). In addition to increased activity within the *rn*+ domain, reporter expression is also stronger in cells outside of the *rn* expression domain, suggesting that this motif has additional Rn-independent functions (Figure 6G). Mutation of conserved motif #2 causes depression throughout the hinge domain, DV boundary, and some cells within the pouch (Figure 6H). When both site #1 and #2 are mutated together, a significant increase in reporter activity is observed throughout the *rn*+ domain (Figure 6I). The strongest derepression, as judged by the more uniform activity along the DV boundary and within the pouch, is observed when all eight motifs are mutated (Figure 6J). These results are consistent with an additive model, where individual motifs in the promoter region each contribute partially to repression of *pdm2* (Figure 6K). Even sites that are more poorly conserved contribute to the final level of repression.

Discussion

In this paper we described a single essential wing enhancer element that is interpreted in two different ways by two paralogous genes, *nubbin* and *pdm2*. This difference results in *nub* being the predominant paralog used during wing development under wild type conditions, while *pdm2* is suppressed by *nub* and *rn*. Upon loss of *nub*, upregulation of *pdm2* permits functional compensation and normal wing development, revealing a redundant function for *pdm2* and *nub* in wing development. As such this system serves as a backup to ensure robust wing development, while keeping the combined Nub/Pdm2 protein levels at the correct level during normal conditions. A function for gene duplicates in providing robustness to genetic and environmental perturbations has been demonstrated in numerous circumstances, but the mechanism by which compensation is achieved is often unknown [7,8].

Evolution of gene regulation in the context of shared enhancers

One potential explanation for the shared expression between duplicated genes, particularly tandem duplicates, is the co-dependence on shared regulatory elements [6,9,10]. Shared regulatory elements have long been implicated in the nested expression patterns of *HOX* paralogs [25]. More recently shared enhancers have been implicated in a wider array of paralogous genes as a result of large-scale reporter screens and chromosome conformation

capture (3C) approaches, which identified enhancers that putatively regulate the promoters of many co-expressed paralogs [6,20,26–28]. While these techniques suggest the widespread utilization of shared enhancers, in most cases functional validation is lacking and the existence of multiple enhancers that separately control both genes cannot be ruled out. Additionally, although there are several models to account for subsequent evolutionary steps following gene and enhancer duplication, it is less clear whether and how context-specific divergence in expression can occur when paralogs are under the control of shared enhancers. Interestingly, both enhancer reporter screens and 3C assays used in the *Drosophila* embryo have suggested the existence of many shared enhancers within the *nub*/*pdm2* that function in both the ectoderm and central nervous system (CNS) [26,27,29]. Thus there may be many shared regulatory elements, in addition to the wing NPW element described here, used by *nub* and *pdm2* throughout development.

Our results provide an interesting comparison with previous work on *nub*/*pdm2* function in the CNS. Although the enhancer(s) governing their expression is not known, *nub* and *pdm2* are co-expressed in the RP2 motor neurons of the embryonic CNS, as well as other CNS cells [15]. Loss of either paralog results in a reduction in the number of RP2 neurons, though *pdm2* has a more pronounced effect, while removal of both genes causes the complete loss of these neurons [15]. Thus in this case the expression of both paralogs is required for complete specification of RP2 neurons, consistent with a dosage subfunctionalization model in which expression of both paralogs has been reduced relative to the ancestral state [30]. In contrast to these observations, here we show that in the majority of wing progenitor cells *pdm2* is actively repressed such that in normal conditions only *nub* is present. The presence of a promoter-localized silencer element requiring *rn* and, via direct or indirect input, *nub*, permits the repression of *pdm2* by *nub.* Importantly, this repression is tissue-specific because it also requires the wing TF, Rn. As a consequence, *nub* does not repress *pdm2* through this silencer outside of the wing, allowing co-expression in other contexts such as the wing hinge and embryonic CNS, where *rn* is not transcribed (BDGP; [31]). Furthermore, the dependence on *nub* for the silencer to function allows *pdm2* to respond to the NPW enhancer when *nub* levels are compromised. Thus, multiple mechanisms can evolve in distinct cell types leading to expression divergence of tandemly duplicate genes.

The role of Rn in repressing *pdm2* in the wing pouch is supported by several lines of evidence: 1) there is a correlation between where *rn* is expressed and where *pdm2* is repressed; 2) a *rn* mutant upregulates *pdm2* in the wing pouch; 3) ectopic Rn in cells that normally express high levels of *pdm2* repress *pdm2*; 4) mutation of Rn binding sites in the *pdm2* promoter derepress its activity; and 5) there is a peak of Rn binding at the *pdm2* promoter. Notably, our Rn ChIP-seq experiments also revealed binding at the *nub* promoter, raising the question of why repression is limited to *pdm2*. One possibility is that there is a second factor that specifically binds to the *pdm2*, but not the *nub,* promoter that is required for repression. Nub, itself, could be such a factor, but because our attempts to map Nub binding *in vivo* were inconclusive, this remains an open question. Alternatively, the Rn binding observed at the *nub* promoter may be non-specific binding to open chromatin, a notion that is supported by the lack of identifiable Rn binding sites at the *nub* promoter.

Flexibility of gene regulation and evolution of silencer elements

The results described here prompt speculation as to how the divergent patterns of *nub*/*pdm2* in the wing may have evolved. Given that *nub*/*pdm2* is a marker for wing development in all winged insects, including species that diverged prior to duplication, it is likely that uniform expression similar to the *nub* pattern is the ancestral state. Thus repression of *pdm2*, through the promoter-proximal silencer element identified here, likely represents an evolutionary novelty that arose at some point post-duplication. The high degree of conservation for two Rn binding sites in the *pdm2* silencer element suggests this divergence may have been fixed shortly after the ancestral gene was duplicated. The acquisition of this silencer permitted conditional separation of *nub*/*pdm2* transcripts while maintaining the ability of *pdm2* to function in a compensatory manner when needed. Alternatively, if duplicated enhancers were used to independently regulate *nub* and *pdm2*, *rn*/*nub* repression of *pdm2* could have been mediated via a *pdm2*-specific enhancer. However, the dependence on a single enhancer in principle necessitates repression occurring independently of the shared enhancer. One mechanism that has been described to mediate promoter selectivity is an inherent preference of enhancers for specific promoter motifs, such as TATA or DPE motifs [32,33] However if such a mechanism was operating for *nub*/*pdm2,* it would be inconsistent with our observation that NPW activates both promoters in part of the distal hinge, and the ability of *pdm2* to respond to the NPW enhancer in the absence of *nub*. The mechanism identified here for conditional repression of *pdm2* thus provides an elegant solution that may be widely applicable to other cases of shared enhancers, or gene regulation in general.

Notably, such promoter-proximal silencers that function to modify distal enhancers have not been identified previously, though transgene experiments have established that repression of enhancers can act over long distances [34]. In contrast, long-range silencer elements have been implicated in previous studies. For example, the analysis of transcriptional regulation of *ebony*, which encodes an enzyme that contributes to yellow cuticle in the developing epidermis of *Drosophila* [35], showed that an upstream enhancer collaborates with a silencer element in the *ebony* intron. An additional silencer is required for sex-specific repression of *ebony* and pigmentation patterns. The repeated evolution of this silencer element through accumulation of inactivating and spatial pattern-affecting mutations in different *Drosophila* species has contributed to species-specific pigmentation patterns [36]. Our analysis suggests that similar acquisition of silencer activity allowed the expression of *pdm2* to diverge from *nub* in the *Drosophila* species that depend on the shared NPW enhancer. Notably, the additive nature of Rn binding sites contributes to spatial differences in repression. We speculate that this is a result of spatial differences in the activating potential of the NPW wing enhancer. In regions where activity is stronger, more repressive input is required, whereas cells where the enhancer is weaker require less repressive input. In further support of this idea, when GMR11F02 is upstream of a synthetic promoter, although it is active throughout the wing domain, its activity is strongest in the distal hinge and DV boundary cells, the same cells that are most sensitive to derepression of the *pdm2* promoter when individual Rn binding sites are mutated. Thus spatial control of silencer activity may gradually evolve through the additive accumulation of repressor binding sites, and the amount of repression will be inversely proportional to the strength of the enhancer. Given prior studies suggesting mutations analyzed in transgenic contexts may be more sensitive

compared to the endogenous locus, future experiments aimed at confirming these results by targeting the endogenous *pdm2* promoter will be useful.

A final question concerns whether the down-regulation of *pdm2* in the wing pouch is important for proper wing development. Evidence in favor of this idea is that *rn* mutants lead to the upregulation of *pdm2* and aberrant wing phenotypes (Figure 5B; [37]), although it is likely that Rn has other functions in wing development in addition to repressing *pdm2*. In addition, ectopic expression of Nub in clones leads to wing defects [38], consistent with the idea that the correct levels of Nub+Pdm2 are important for wing development. Our attempts to increase Pdm2 levels led to lethality, thus preventing us from addressing this question. In the future, experiments that upregulate *pdm2* more subtly, for example by mutating multiple Rn binding sites at the endogenous *pdm2* promoter, may be needed to definitively answer this question.

STAR Methods

Resource Availability

Lead contact—Further information and requests for resources and reagents should be directed to and will be fulfilled by the Lead Contact, Richard Mann (rsm10@columbia.edu).

Materials availability—Fly lines and reporter constructs generated by this study will be shared by the lead contact upon request.

Data and code availability

- All ATAC-seq, RNA-seq, and ChIP-seq data have been deposited at GEO and are publicly available as of the date of publication. Accession numbers are listed in the key resources table. Microscopy data reported in this paper will be shared by the lead contact upon request.
- This paper does not report original code
- Any additional information required to reanalyze the data reported in this paper is available from the lead contact upon request.

Experimental Model and Subject Details

Experimental model for this study was the vinegar fly Drosophila melanogaster. A full list of strains used in the paper is included in the Key Resource Table. Unless otherwise described (See Method Details section), flies were maintained at 25C on cornmeal food using standard laboratory techniques.

Method Details

Reporter constructs—The GMR11F02 reporter construct was generated previously by inserting the genomic coordinates:chr2L:12,634,617–12,638,421 (dm6 assembly) into the pBPGUw vector containing the Drosophila synthetic core promoter (DSCP) upstream of the Gal4 coding sequence. This construct was re-injected into the attP40 landing site (this study) by Rainbow Transgenic injection service. To exchange the DSCP with the endogenous *pdm2*

promoter, the sequence was synthesized either corresponding to the reference genome or with indicated *rn* motif mutants by Genewiz containing restriction sites for FseI and KpnI (see Key Resource table). The DSCP was removed from GMR11F02 using the FseI and KpnI restriction sites, and replaced with the *pdm2* promoter. All plasmids were inserted into the attp40 landing site for this study using standard phiC31 injections performed by Rainbow Transgenic Flies injection service

Generation of NPW enhancer deletions—Preparation of materials for Cas9-mediated deletions were performed as previously described [39]. gRNA target sites (two sites per deletion) were predicted using the flyCRISPR bioinformatic tool and subsequently sanger sequencing on the genomic region surrounding target sites was performed to confirm their presence in the Cas9-expressing stock (Rainbow Transgenic Flies: line#55821). gRNAs (see Key Resource table) were cloned into the pCFD5 vector. For donor constructs the TVattp-Pax-Cherry was used and homology arms were inserted using standard restriction enzyme mediated cloning with primers listed (see Key Resource table). For the NPW small and large deletion the same gRNA and Homology arm on one side was used. Injection was carried out by Rainbow Transgenic using the Cas9-expressing fly strain. Screening for successful deletion was performed using Pax-Cherry expression, and subsequently gDNA was extracted and sanger sequencing performed to confirm boundaries of Cas9-mediated lesions. Stocks were established from lines containing the correct targeting and subsequently flies were crossed to a Cre-expression strain to remove Pax-Cherry marker using flanking LoxP sites contained in the targeting vector. The resulting stocks contain a single attP and LoxP site in place of the deleted fragment.

Immunohistochemistry—Immunohistochemistry was performed using standard practices as previously described [24].

Ectopic expression of Rotund—To make Rn-expressing clones female flies from a *yw hs-flp*$^{1.22}$*;UAS-FRT.STOP.FRT-Gal4* strain were crossed to males containing *UAS-Rn* (Bloomington:7403). 72 hours after egg laying, larvae from this cross were placed at 37C for 10 minutes to induce clones and analyzed 48 hours later by antibody staining of late 3rd instar.

ChIP-seq—ChIP-seq was performed as described [24] previously on 3rd instar larvae containing a GFP knock-in of the endogenous *rn* coding sequence [22]. Briefly, 3rd instar larval heads were dissected and inverted in PBS on ice. Heads were fixed for 20 minutes in 1.8% PFA in crosslinking medium (10 mM HEPES, pH=8.0; 100 mM NaCl; 1 mM EDTA, pH=8.0; 0.5 mM EGTA, pH=8.0) at room-temperature with rotation, and subsequently quenched (Quench solution: 1xPBS; 125 mM glycine; 0.1% Triton X-100). Fixed-heads were then washed 2X in buffer A (10 mM HEPES, pH=8.0; 10 mM EDTA, pH=8.0; 0.5 mM EGTA, pH=8.0, 0.25 % Triton X-100) and 2X buffer B (10 mM HEPES, pH=8.0; 200 mM NaCl; 1 mM EDTA, pH=8.0; 0.5 mM EGTA, pH=8.0; 0.01% Triton X-100) 10 minutes each at 4°C. Wing discs were then dissected and placed in sonication buffer (10 mM HEPES, pH = 8.0; 1 mM EDTA, pH = 8.0; 0.5 mM EGTA, pH = 8.0, 0.1 % SDS). Chromatin sonication was performed using a Covaris S2 instrument at settings (105W; 2 % Duty; 15 minutes).

Sonicated chromatin was brought to 1X mild-RIPA (10 mM Tris-HCl, pH=8.0; 1 mM EDTA, pH=8.0; 150 mM NaCl; 1% Triton X-100) concentration and pre-cleared with Dynabeads for 1 hour at 4 °C with rotation. Pre-clearing beads were removed and antibody was added for incubation overnight. Dynabeads were added and incubated for 3 hrs. Bead bound antibody-chromatin complexes were washed as follows 2X RIPA LS (10 mM Tris-HCl, pH=8.0; 1 mM EDTA, pH=8.0; 150 mM NaCl; 1% Triton X-100; 0.1 % SDS; 0.1 % DOC), 2X RIPA HS (10 mM Tris-HCl, pH=8.0; 1 mM EDTA, pH=8.0; 500 mM NaCl; 1% Triton X-100; 0.1 % SDS; 0.1 % DOC), 1X LiCl (10mM Tris-HCl, pH=8.0; 1 mM EDTA, pH=8.0; 250 mM LiCl; 0.5 % IGEPAL CA-630; 0.5 % DOC), 1X TE (10 mM Tris-HCl, pH=8.0; 1 mM EDTA, pH=8.0). Samples were then treated with RNAse and proteinase K, and chromatin was isolated using phenol-chloroform.

An anti-GFP (ab290, Abcam; 1:300 dilution for IP) was used to perform chromatin precipitation. ChIP-seq libraries were made following the NEBnext UltraII kit (NEB) and associated protocol. Libraries were sequenced using a 75-cycle high output with single end sequencing using an Illumina Nextseq. Two replicates were performed.

RNA-seq—For *nub*^{1} and wild type control samples, RNA was extracted from dissected whole discs using TRIzol and purified using Zymo Direct-zol RNA Microprep kit. Ten discs were used for each replicate. Libraries were prepared using NEBnext Ultra II Directional RNA-seq kit and sequenced using a 75-cycle single-end high output run with an Illumina Nextseq. Three replicates were performed for each experiment.

ATAC-seq—For *nub*^{1} and wild type control samples, whole wing discs were dissected and subjected to the ATAC-seq protocol as previously described [19,40]. Three discs were used for each replicate. Libraries were sequenced using a 75-cycle high output with paired end sequencing using an Illumina Nextseq. Two replicates were performed for all ATAC-seq experiments.

Somatic CRISPR—To generate wing discs with somatic *nub* knockout, female flies containing *UAS-Cas9.M* [41];*hdc.G4* were crossed to flies containing *UAS-nub.gRNA* (containing two gRNAs within the pCFD6 plasmid targeting coding exons shared in all *nub* isoforms, Vienna Drosophila Resource Center: 341604). When performed in *pdm2* null background: *UAS-Cas9.M,pdm2*^{E46}*;hdc.G4* and *pdm2*^{E46}*,UAS-nub.gRNA* stocks were used.

Quantification and Statistical Analysis

RNA-seq data processing—Reads were mapped using HISAT2 to the dm6 genome assembly. Mapped reads were then filtered for map quality using SAMtools [42]. Genome-track files were created using Deeptools (BamCoverage; RPGC normalization) [43].

ATAC-seq data processing—Reads were mapped using Bowtie2 to the dm6 genome assembly. Mapped reads were then filtered for map quality using SAMtools [42]and duplicates (Picard MarkDuplicates). Genome-track files were created using Deeptools (BamCoverage; RPGC normalization) [43].

ChIP-seq data processing—Reads were mapped using Bowtie2 to the dm6 genome assembly. Mapped reads were then filtered for map quality using SAMtools [42] and duplicates (Picard MarkDuplicates). Peaks were called using MACS2 callpeak function with default parameters [44]. Genome-track files were created using Deeptools (BamCoverage; RPKM normalization)[43].

Motif analysis—*De novo* motifs were discovered using Homer (findmotifsgenome.pl)[45]. For ATAC-seq data the entire peak was used to search for enriched motifs (option: -size given) and all ATAC peaks (minus the queried group) were used to calculate background enrichment. For ChIP-seq a default 200bp window around the peak center was used.

Supplementary Material

Refer to Web version on PubMed Central for supplementary material.

Acknowledgements:

We would like to thank all members of the Mann lab and Peter Andolfatto for helpful discussions during the course of this project and to David Stern for comments on the manuscript; the Bloomington Drosophila Stock Center for reagents; Flybase for information related to alleles used here; Pelin Volkan for the *rn*-GFP stock; Wes Grueber for fly reagents; Cyrille Alexandre and J.P Vincent for CRISPR targeting reagents; Fillip Port for CRISPR fly reagents. This work was supported by NIH grant R35GM118336 awarded to R.S.M.

Data availability

All imaging data and fly stocks associated with this study are available upon request. Genomic data generated previously corresponding to sorted wing and haltere imaginal disc populations is available within the GEO database with the accession **GSE166714**. Sequencing data generated from this study using RNA-seq (yw and nub^{1}), ATAC-seq (yw and nub^{1}), and ChIP-seq (*rn*-GFP) is available under accession **GSE203208**.

References

1. Ohno S (1970). Evolution by Gene Duplication (Springer Berlin Heidelberg).
2. Force A, Lynch M, Pickett FB, Amores A, Yan YL, and Postlethwait J (1999). Preservation of duplicate genes by complementary, degenerative mutations. Genetics 151, 1531–1545. [PubMed: 10101175]
3. Lynch M, O'Hely M, Walsh B, and Force A (2001). The probability of preservation of a newly arisen gene duplicate. Genetics 159, 1789–1804. [PubMed: 11779815]
4. Lynch M, and Force A (2000). The probability of duplicate gene preservation by subfunctionalization. Genetics 154, 459–473. [PubMed: 10629003]
5. Kuzmin E, VanderSluis B, Nguyen Ba AN, Wang W, Koch EN, Usaj M, Khmelinskii A, Usaj MM, van Leeuwen J, Kraus O, et al. (2020). Exploring whole-genome duplicate gene retention with complex genetic interaction analysis. Science 368, eaaz5667. [PubMed: 32586993]
6. Lan X, and Pritchard JK (2016). Coregulation of tandem duplicate genes slows evolution of subfunctionalization in mammals. Science 352, 1009–1013. [PubMed: 27199432]
7. Gu Z, Steinmetz LM, Gu X, Scharfe C, Davis RW, and Li W-H (2003). Role of duplicate genes in genetic robustness against null mutations. Nature 421, 63–66. [PubMed: 12511954]
8. Osterwalder M, Barozzi I, Tissières V, Fukuda-Yuzawa Y, Mannion BJ, Afzal SY, Lee EA, Zhu Y, Plajzer-Frick I, Pickle CS, et al. (2018). Enhancer Redundancy Allows for Phenotypic Robustness in Mammalian Development. Nature 554, 239–243. [PubMed: 29420474]

9. Quintero-Cadena P, and Sternberg PW (2016). Enhancer Sharing Promotes Neighborhoods of Transcriptional Regulation Across Eukaryotes. G3 GenesGenomesGenetics 6, 4167–4174.
10. Williams EJB, and Bowles DJ (2004). Coexpression of Neighboring Genes in the Genome of Arabidopsis thaliana. Genome Res. 14, 1060–1067. [PubMed: 15173112]
11. Baudouin-Gonzalez L, Santos MA, Tempesta C, Sucena É, Roch F, and Tanaka K (2017). Diverse Cis-Regulatory Mechanisms Contribute to Expression Evolution of Tandem Gene Duplicates. Mol. Biol. Evol. 34, 3132–3147. [PubMed: 28961967]
12. Cifuentes FJ, and García-Bellido A (1997). Proximo–distal specification in the wing disc of Drosophila by the nubbin gene. Proc. Natl. Acad. Sci. 94, 11405–11410. [PubMed: 9326622]
13. Corty MM, Tam J, and Grueber WB (2016). Dendritic diversification through transcription factor-mediated suppression of alternative morphologies. Development 143, 1351–1362. [PubMed: 27095495]
14. Ng M, Diaz-Benjumea FJ, and Cohen SM (1995). Nubbin encodes a POU-domain protein required for proximal-distal patterning in the Drosophila wing. Dev. Camb. Engl. 121, 589–599.
15. Yeo SL, Lloyd A, Kozak K, Dinh A, Dick T, Yang X, Sakonju S, and Chia W (1995). On the functional overlap between two Drosophila POU homeo domain genes and the cell fate specification of a CNS neural precursor. Genes Dev. 9, 1223–1236. [PubMed: 7758947]
16. Averof M, and Cohen SM (1997). Evolutionary origin of insect wings from ancestral gills. Nature 385, 627–630. [PubMed: 9024659]
17. Tomoyasu Y, Arakane Y, Kramer KJ, and Denell RE (2009). Repeated Co-options of Exoskeleton Formation during Wing-to-Elytron Evolution in Beetles. Curr. Biol. 19, 2057–2065. [PubMed: 20005109]
18. López-Varea A, Vega-Cuesta P, Ruiz-Gómez A, Ostalé CM, Molnar C, Hevia CF, Martín M, Organista MF, de Celis J, Culí J, et al. (2021). Genome-wide phenotypic RNAi screen in the Drosophila wing: phenotypic description of functional classes. G3 GenesGenomesGenetics 11, jkab349.
19. Buenrostro JD, Giresi PG, Zaba LC, Chang HY, and Greenleaf WJ (2013). Transposition of native chromatin for fast and sensitive epigenomic profiling of open chromatin, DNA-binding proteins and nucleosome position. Nat. Methods 10, 1213–1218. [PubMed: 24097267]
20. Jory A, Estella C, Giorgianni MW, Slattery M, Laverty TR, Rubin GM, and Mann RS (2012). A Survey of 6,300 Genomic Fragments for cis-Regulatory Activity in the Imaginal Discs of Drosophila melanogaster. Cell Rep. 2, 1014–1024. [PubMed: 23063361]
21. St Pierre SE, Galindo MI, Couso JP, and Thor S (2002). Control of Drosophila imaginal disc development by rotund and roughened eye: differentially expressed transcripts of the same gene encoding functionally distinct zinc finger proteins. Development 129, 1273–1281. [PubMed: 11874922]
22. Li Q, Barish S, Okuwa S, and Volkan PC (2015). Examination of Endogenous Rotund Expression and Function in Developing Drosophila Olfactory System Using CRISPR-Cas9–Mediated Protein Tagging. G3 Genes Genomes Genet. 5, 2809–2816.
23. Lewis EB (1978). A gene complex controlling segmentation in Drosophila. Nature 276, 565–570. [PubMed: 103000]
24. Loker R, Sanner JE, and Mann RS (2021). Cell-type-specific Hox regulatory strategies orchestrate tissue identity. Curr. Biol. CB 31, 4246–4255.e4. [PubMed: 34358443]
25. Gould A, Morrison A, Sproat G, White RA, and Krumlauf R (1997). Positive cross-regulation and enhancer sharing: two mechanisms for specifying overlapping Hox expression patterns. Genes Dev. 11, 900–913. [PubMed: 9106661]
26. Ghavi-Helm Y, Zhao B, and Furlong EEM (2016). Chromatin Immunoprecipitation for Analyzing Transcription Factor Binding and Histone Modifications in Drosophila. Methods Mol. Biol. Clifton NJ 1478, 263–277.
27. Kvon EZ, Kazmar T, Stampfel G, Yáñez-Cuna JO, Pagani M, Schernhuber K, Dickson BJ, and Stark A (2014). Genome-scale functional characterization of Drosophila developmental enhancers in vivo. Nature 512, 91–95. [PubMed: 24896182]

28. Symmons O, Uslu VV, Tsujimura T, Ruf S, Nassari S, Schwarzer W, Ettwiller L, and Spitz F (2014). Functional and topological characteristics of mammalian regulatory domains. Genome Res. 24, 390–400. [PubMed: 24398455]
29. Ross J, Kuzin A, Brody T, and Odenwald WF (2015). cis-regulatory analysis of the Drosophila pdm locus reveals a diversity of neural enhancers. BMC Genomics 16.
30. Gout J-F, and Lynch M (2015). Maintenance and Loss of Duplicated Genes by Dosage Subfunctionalization. Mol. Biol. Evol. 32, 2141–2148. [PubMed: 25908670]
31. Tomancak P, Beaton A, Weiszmann R, Kwan E, Shu S, Lewis SE, Richards S, Ashburner M, Hartenstein V, Celniker SE, et al. (2002). Systematic determination of patterns of gene expression during Drosophila embryogenesis. Genome Biol. 3, RESEARCH0088. [PubMed: 12537577]
32. Juven-Gershon T, Hsu J-Y, and Kadonaga JT (2008). Caudal, a key developmental regulator, is a DPE-specific transcriptional factor. Genes Dev. 22, 2823–2830. [PubMed: 18923080]
33. Ling J, Umezawa KY, Scott T, and Small S (2019). Bicoid-Dependent Activation of the Target Gene hunchback Requires a Two-Motif Sequence Code in a Specific Basal Promoter. Mol. Cell 75, 1178–1187.e4. [PubMed: 31402096]
34. Cai HN, Arnosti DN, and Levine M (1996). Long-range repression in the Drosophila embryo. Proc. Natl. Acad. Sci. U. S. A. 93, 9309–9314. [PubMed: 8790326]
35. Rebeiz M, Pool JE, Kassner VA, Aquadro CF, and Carroll SB (2009). Stepwise Modification of a Modular Enhancer Underlies Adaptation in a Drosophila Population. Science 326, 1663–1667. [PubMed: 20019281]
36. Johnson WC, Ordway AJ, Watada M, Pruitt JN, Williams TM, and Rebeiz M (2015). Genetic Changes to a Transcriptional Silencer Element Confers Phenotypic Diversity within and between Drosophila Species. PLoS Genet. 11, e1005279. [PubMed: 26115430]
37. Cavener DR, Otteson DC, and Kaufman TC (1986). A Rehabilitation of the Genetic Map of the 84b-D Region in DROSOPHILA MELANOGASTER. Genetics 114, 111–123. [PubMed: 3095179]
38. Neumann CJ, and Cohen SM (1998). Boundary Formation in Drosophila Wing: Notch Activity Attenuated by the POU Protein Nubbin. Science 281, 409–413. [PubMed: 9665883]
39. Alexandre C, Baena-Lopez A, and Vincent J-P (2014). Patterning and growth control by membrane-tethered Wingless. Nature 505, 180–185. [PubMed: 24390349]
40. Jacobs J, Atkins M, Davie K, Imrichova H, Romanelli L, Christiaens V, Hulselmans G, Potier D, Wouters J, Taskiran II, et al. (2018). The transcription factor Grainy head primes epithelial enhancers for spatiotemporal activation by displacing nucleosomes. Nat. Genet. 50, 1011–1020. [PubMed: 29867222]
41. Port F, Strein C, Stricker M, Rauscher B, Heigwer F, Zhou J, Beyersdörffer C, Frei J, Hess A, Kern K, et al. (2020). A large-scale resource for tissue-specific CRISPR mutagenesis in Drosophila. eLife 9, e53865. [PubMed: 32053108]
42. Li H, Handsaker B, Wysoker A, Fennell T, Ruan J, Homer N, Marth G, Abecasis G, Durbin R, and 1000 Genome Project Data Processing Subgroup (2009). The Sequence Alignment/Map format and SAMtools. Bioinforma. Oxf. Engl. 25, 2078–2079.
43. Ramírez F, Ryan DP, Grüning B, Bhardwaj V, Kilpert F, Richter AS, Heyne S, Dündar F, and Manke T (2016). deepTools2: a next generation web server for deep-sequencing data analysis. Nucleic Acids Res. 44, W160–W165. [PubMed: 27079975]
44. Zhang Y, Liu T, Meyer CA, Eeckhoute J, Johnson DS, Bernstein BE, Nusbaum C, Myers RM, Brown M, Li W, et al. (2008). Model-based Analysis of ChIP-Seq (MACS). Genome Biol. 9, R137. [PubMed: 18798982]
45. Heinz S, Benner C, Spann N, Bertolino E, Lin YC, Laslo P, Cheng JX, Murre C, Singh H, and Glass CK (2010). Simple combinations of lineage-determining transcription factors prime cis-regulatory elements required for macrophage and B cell identities. Mol. Cell 38, 576–589. [PubMed: 20513432]
46. Calleja M, Moreno E, Pelaz S, and Morata G (1996). Visualization of Gene Expression in Living Adult Drosophila. Science 274, 252–255. [PubMed: 8824191]

47. Agnel M, Kerridge S, Vola C, and Griffin-Shea R (1989). Two transcripts from the rotund region of Drosophila show similar positional specificities in imaginal disc tissues. Genes Dev. 3, 85–95. [PubMed: 2496007]

48. Wilson C, Pearson RK, Bellen HJ, O'Kane CJ, Grossniklaus U, and Gehring WJ (1989). P-element-mediated enhancer detection: an efficient method for isolating and characterizing developmentally regulated genes in Drosophila. Genes Dev. 3, 1301–1313. [PubMed: 2558051]

49. Port F, and Bullock SL (2016). Augmenting CRISPR applications in Drosophila with tRNA-flanked Cas9 and Cpf1 sgRNAs. Nat. Methods 13, 852–854. [PubMed: 27595403]

50. Langmead B, and Salzberg SL (2012). Fast gapped-read alignment with Bowtie 2. Nat. Methods 9, 357–359. [PubMed: 22388286]

Highlights

- The classical *nub*^{1} allele of *Drosophila* is a deletion of a transcriptional enhancer
- This enhancer is required for expression of both *nub* and *pdm2* in wing discs
- *pdm2* and *nub* expression patterns differ due to repression through the *pdm2* promoter
- Repression of *pdm2* is limited to part of the wing due to input from *nub* and *rotund*

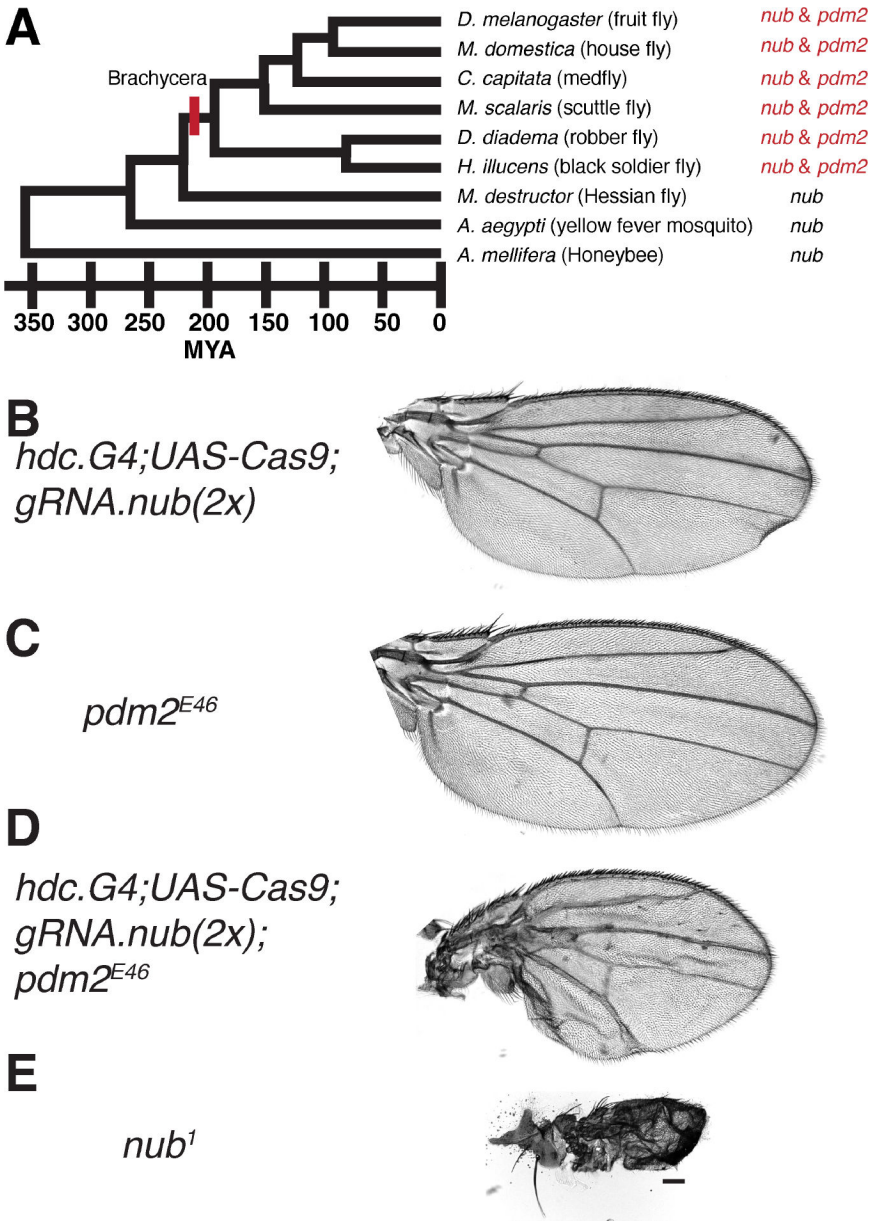

Figure 1. Functional redundancy of *nubbin* and *pdm2* during wing development

(**A**) Duplication of an ancestral proto *nub*/*pdm2* gene occurred in the Dipteran lineage near the base of divergence within the Brachycera suborder. Time span shown below is approximate millions of years ago (MYA).

(**B-E**) Adult wing morphology with the following conditions: (**B**) Somatic CRISPR targeting *nubbin* coding exons with two gRNAs (**C**) *pdm2* truncated allele: $pdm2^{E46}$ (**D**) Somatic CRISPR targeting *nubbin* coding exons with two gRNAs in a $pdm2^{46}$ background. The resulting phenotype is a partial disruption of wing morphology due to the mosaic nature of somatic CRISPR (see Figure S1C). (**E**) nub^{1} allele. Scale bar is 100um.

See also Figure S1.

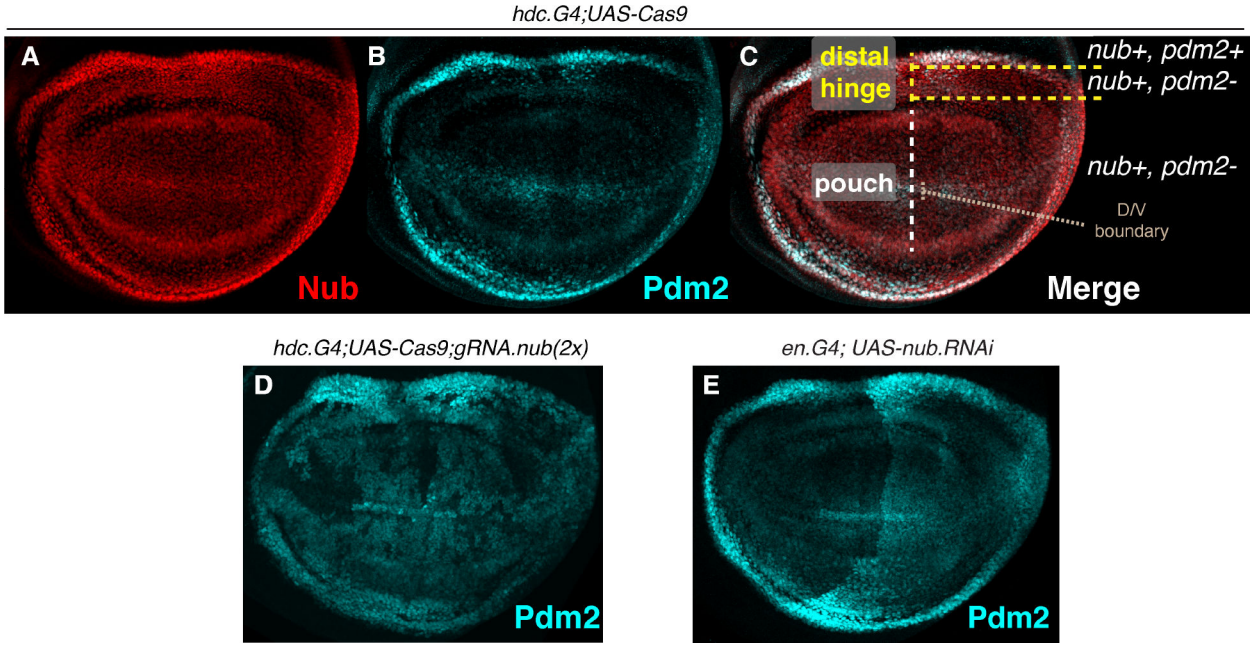

Figure 2. Expression of Nub and Pdm2 in the developing wing in normal and *nub* loss-of-function conditions

(**A**) Expression of Nub protein in the wing imaginal disc. Note that the anti-Nub antibody recognizes both Nub and Pdm2 (**B**) Expression of Pdm2 in the wing imaginal disc. High levels of Pdm2 protein are limited to the peripheral cells of the appendage domain. (**C**) Merged Nub/Pdm2 expression with relevant domains indicated. (**D**) Expression of Pdm2 in the wing imaginal disc upon targeting of *nub* with somatic CRISPR (compare with (**B**), which expresses Cas9 but no gRNA). Pdm2 levels are elevated in the majority of cells within the central domain of the appendage domain. Patches of cells with lower Pdm2 levels can be observed that are likely a result of incomplete Nub knockout, as the somatic CRISPR produces a mosaic loss-of-function (see Figure S1C). (**E**) RNAi knockdown of *nub* in the posterior compartment with *engrailed-Gal4* leads to upregulation of Pdm2; note that the endogenous levels of Pdm2 in the adjacent anterior compartment serve as an internal control.

See also Figure S2.

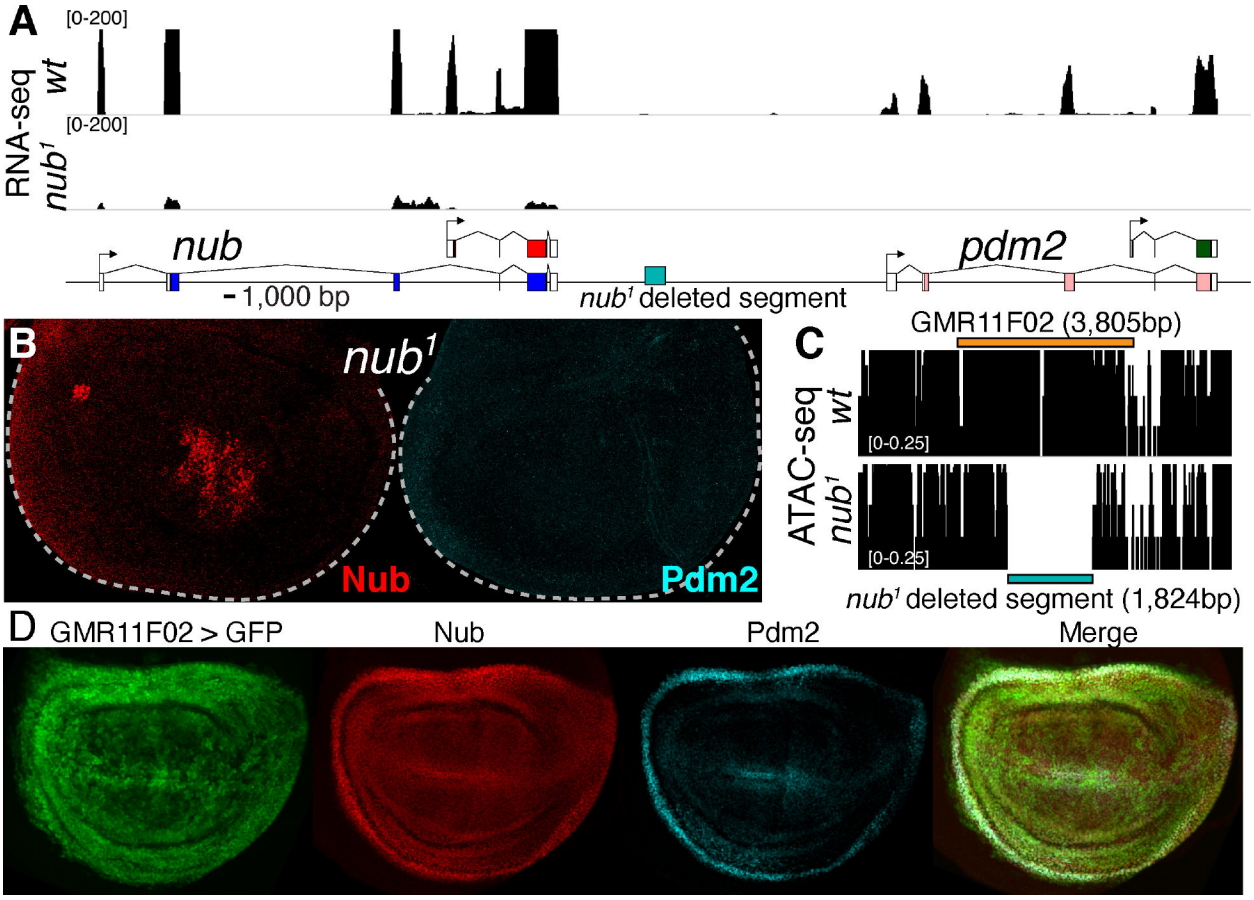

Figure 3. Additional characterization of the classic *nub*^{1} allele

(**A**) Transcriptomic analysis of the *nub*^{1} wing discs within the *nub*/*pdm2* genomic locus. Both *nub* and *pdm2* transcripts are reduced relative to the wild type (wt) *yw* strain. (**B**) Protein levels of Nub (left) and Pdm2 (right) in *nub*^{1} wing discs are reduced. Some staining of Nub is observed in the central pouch, as previously described, and consistent with the RNA-seq analysis. Discs are outlined with a dashed line. (**C**) ATAC-seq analysis revealed a lesion of DNA (blue box) in the intergenic region between *nub* and *pdm2* (see blue box in (**A**)). The location of reporter GMR11F02 overlapping this region is indicated (orange box). (**D**) Expression of a reporter construct containing GMR11F02 demonstrates that this segment is a wing domain enhancer overlapping the expression of Nub.

See also Figure S3.

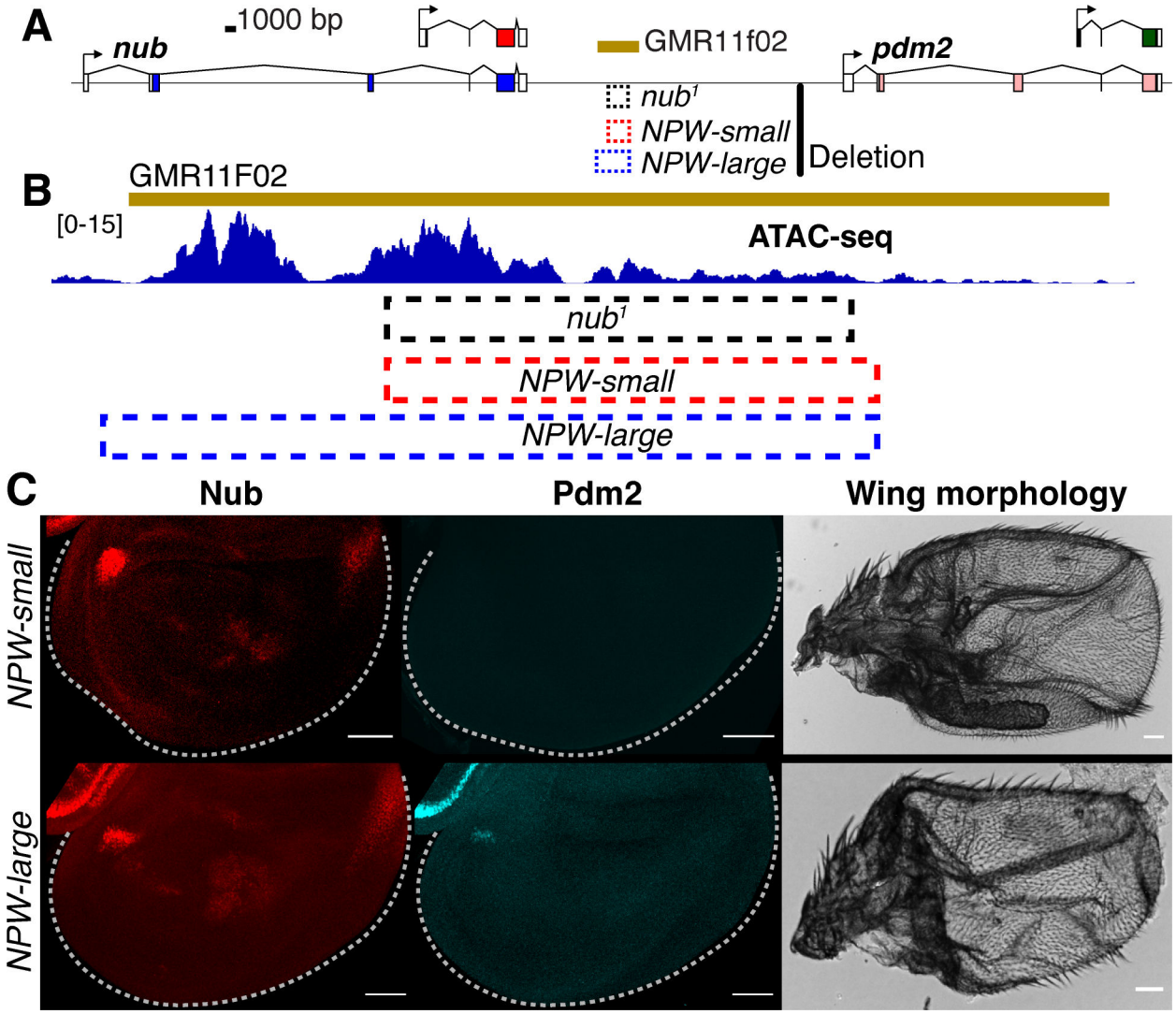

Figure 4. NPW is an essential wing enhancer shared by *nub* and *pdm2*

(**A**) Deletions corresponding to the lesion observed in the *nub*^{1} and CRISPR-mediated alleles (*NPW-small* and *NPW-large*) generated in this study within the *nub*/*pdm2* genomic locus are indicated. (**B**) Accessible chromatin in wild type wing discs in the genomic region overlapping GMR11F02. A large open chromatin peak is contained within the *nub*^{1} lesion and an additional adjacent peak is contained within the GMR11F02 region. The *NPW-small* deletion coordinates mimic the *nub*^{1} lesion while the NPW-large deletion removes both open chromatin regions. (**C**) *NPW-small* (top) and *NPW-large* deletion (bottom) phenocopies the *nub*^{1} allele both in regards to Nub and Pdm2 protein expression (left) and phenotype (right). Discs are outlined with a dashed line. Scale bar is 50 μm.

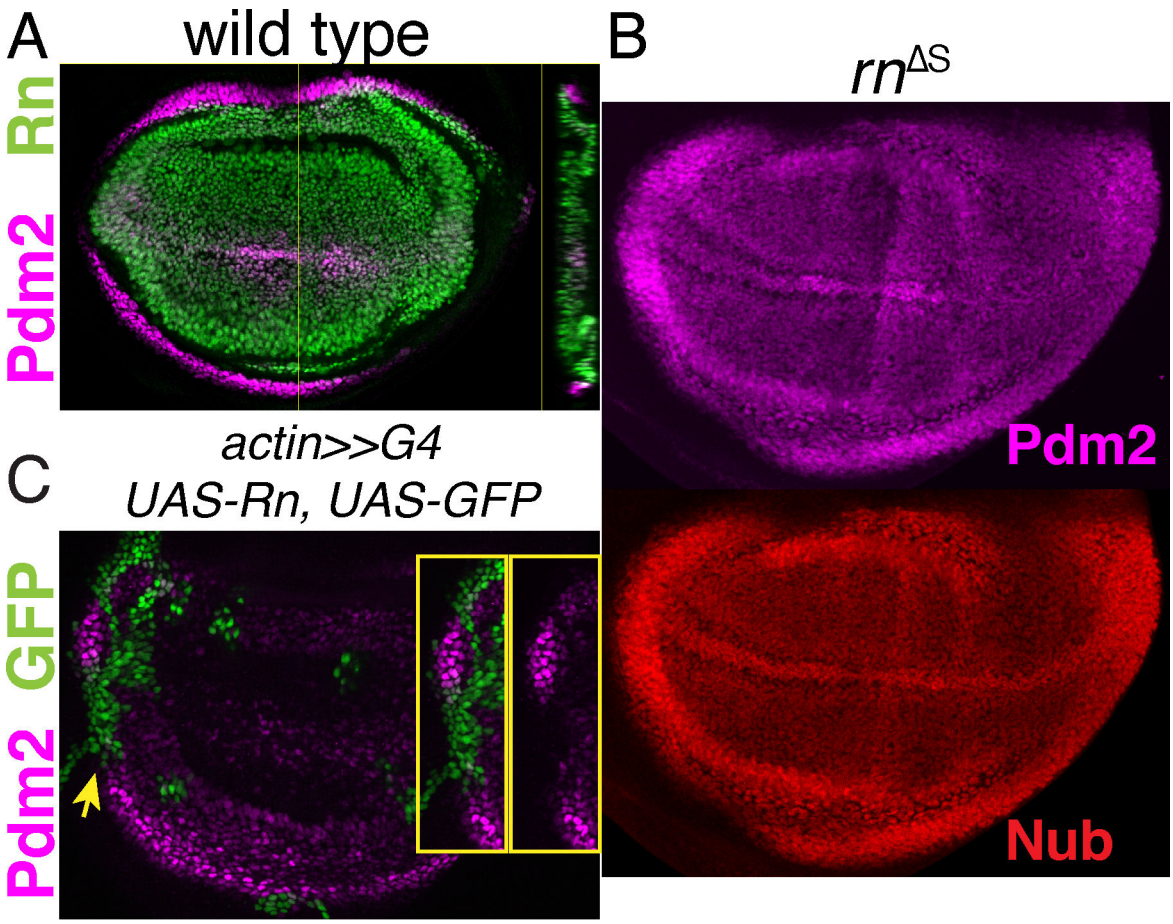

Figure 5. Repression of *pdm2* by Rotund

(A) *rotund*-GFP tagged allele (green) is expressed in the central wing domain adjacent to the Pdm2-high (magenta) wing periphery. Transverse section is shown (right). (**B**) Pdm2 (magenta) is derepressed in a *rn* null wing disc. (**C**) Heat shock induced clones ectopically expressing *rn* (visualized by GFP) cause repression of Pdm2 in the peripheral hinge domain. See also Figure S4.

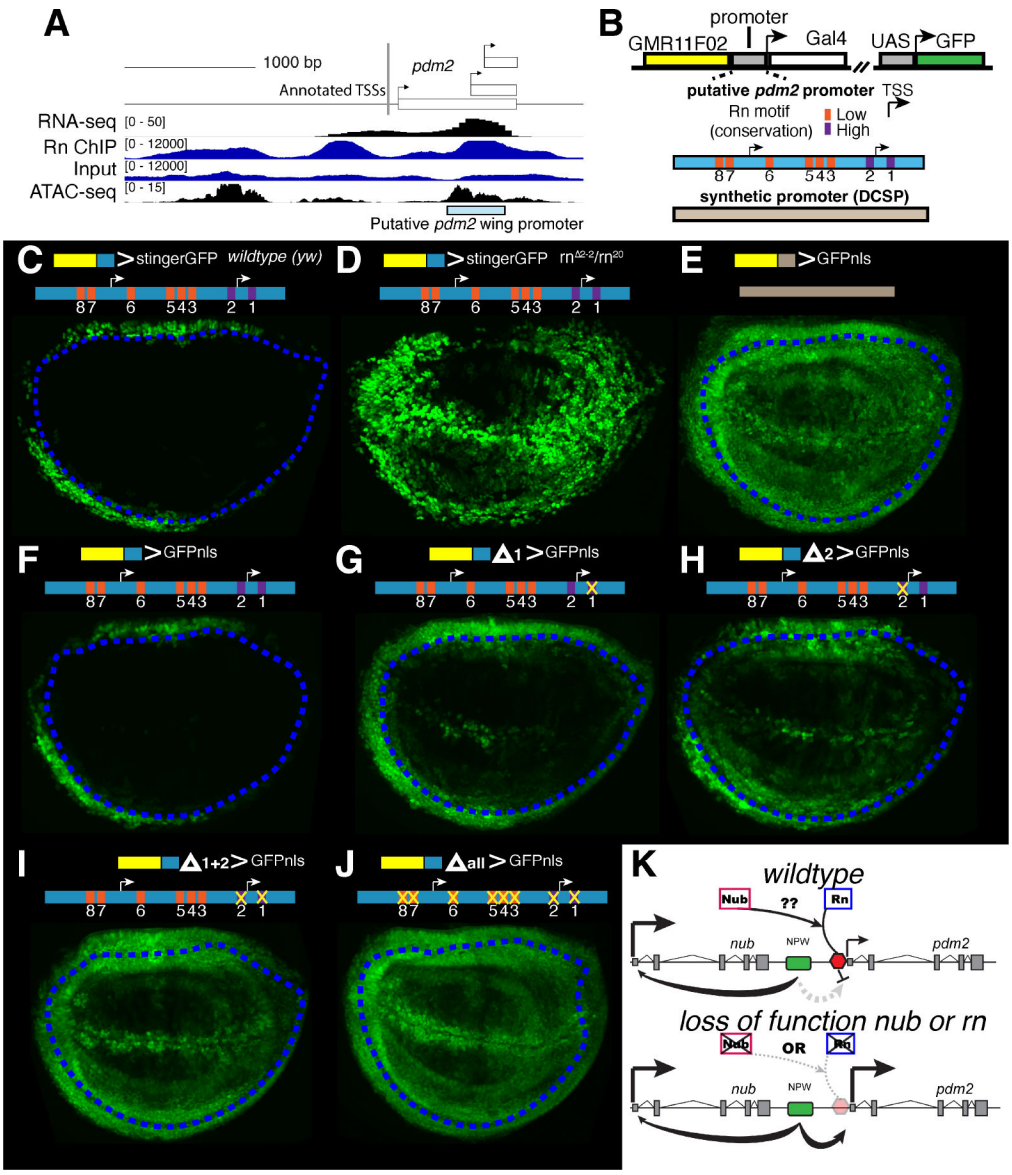

Figure 6. Rn directly represses *pdm2* through a promoter-localized silencer element

(A) *pdm2* promoter region with genome browser tracks of wing disc RNA-seq (top track), ChIP-seq enrichment of Rn and associated input control (second and third track, respectively) and ATAC-seq accessible chromatin (bottom track). Predicted wing promoter is indicated (blue box). (**B**) Diagram of enhancer-reporter constructs and different promoters used: putative *pdm2* promoter (blue) and Drosophila Synthetic Core Promoter (DSCP, tan). Consensus Rn binding motifs within the putative *pdm2* promoter shown and whether they are located in highly conserved sequence blocks is indicated by purple (yes) or orange (no). (**C-D**) Reporter expression from constructs containing GMR11F02 upstream of the *pdm2* promoter driving a UAS-GFPstinger(GFPnls variant) in wild type(**C**) and *rn* null(**D**) wing discs. Note that the peripheral hinge domain (where *pdm2* is normally expressed) is deleted in the *rn* null background. Therefore observed expression is likely all a result of derepression. (**E-J**) Reporter (UAS-GFPnls) expression of constructs containing GMR11F02

upstream of different promoter variants: (**E**) DSCP (**F**) wild type *pdm2* promoter (**G**) *pdm2* promoter: Rn site 1 mutant (**H**) *pdm2* promoter: Rn site 2 mutant (**I**) *pdm2* promoter: Rn site 1+2 mutant (**J**) *pdm2* promoter: All Rn sites mutant. Distal limit of Pdm2 protein expression is indicated by blue dashed line in all images with the exception of (**D**) where Pdm2 is uniformly expressed. (**K**) Model for paralog-specific suppression of NPW activity in wild type and mutant (*nub* or *rn*) conditions.
See also Figure S5.

KEY RESOURCES TABLE

REAGENT or RESOURCE	SOURCE	IDENTIFIER
Antibodies		
Rat anti-Pdm2	abcam	ab201325
Mouse anti-Nub	Developmental Studies Hybridoma Bank	2D459
Rabbit anti-GFP	abcam	Ab209
Critical commercial assays		
NEB Ultra DNA library prep kit Ultra II	NEB	E7645S
Nextera DNA Library Preparation Kit	Illumina	FC-404-2005
NEB Ultra RNA Directional library prep kit Ultra II	NEB	E7760S
Deposited data		
Raw and analyzed data	This study	GEO: GSE203208
Experimental models: Organisms/strains		
Drosophila melanogaster: nub.Gal4	[46]	N/A
Drosophila melanogaster: en.Gal4	n/a	BDSC: 30564
Drosophila melanogaster: hdc.Gal4		
Drosophila melanogaster: pdm2[E46]	[15]	N/A
Drosophila melanogaster: UAS-GFP.nls	Blooming Drosophila Stock Center	BDSC: 4776
Drosophila melanogaster: UAS-Stinger	Blooming Drosophila Stock Center	BDSC: 84277
Drosophila melanogaster: UAS-nub.gRNA(2x)	[41]	VDRC: 341604
Drosophila melanogaster: UAS-cas9M	[41]	N/A
Drosophila melanogaster: UAS-nub.RNAi	Vienna Drosophila Resource Center	VDRC: 105044
Drosophila melanogaster: GMR11F02.Gal4	[20]	BDSC: 49828
Drosophila melanogaster: Rn-GFP fusion	[22]	
Drosophila melanogaster: Rn^{deltaS}	Stefan Thor	BDSC: 8142
Drosophila melanogaster: Rn^{20}	[47]	BDSC: 7409
Drosophila melanogaster: $Rn^{delta2-2}$	[48]	BDSC: 7410
Drosophila melanogaster: NPW_del_small	This Study	N/A
Drosophila melanogaster: NPW_del_large	This Study	N/A
Drosophila melanogaster: GMR11F02.pdm2prom.Gal4	This Study	N/A
Drosophila melanogaster: yw	Wildtype lab strain	N/A
Oligonucleotides		
NPW-small_gRNA#1: TGGGCTACTGTTGGGAGACC	This study	N/A
NPW-small_gRNA#2: TTATTTCATAAAGCTCATAA	This study	N/A

REAGENT or RESOURCE	SOURCE	IDENTIFIER
NPW-small_left_homology_Forward: ttttGCGGCCGCGTTTGTCTCGGGCACCTCTAC	This study	N/A
NPW-small_left_homology_Reverse: ttttGGTACCACCCGGAGCTCTTGTCCC	This study	N/A
NPW-small_right_homology_Forward: ttttGACGTCTGAGCTTTATGAAATAAAGACTTTATATA G	This study	N/A
NPW-small_right_homology_Reverse: ttttACCGGTCTCGTAGGTGATATGTGTCATC	This study	N/A
NPW-large_gRNA#1: GAGGCGTTCTGAGAAGTGTT	This study	N/A
NPW-large_gRNA#2: TTATTTCATAAAGCTCATAA	This study	N/A
NPW-large_left_homology_Forward: ttttGCGGCCGCCATAATAACCCTACCCGAAAGTCC	This study	N/A
NPW-large_left_homology_Reverse: ttttGGTACCACTTCTCAGAACGCCTCAG	This study	N/A
NPW-large_right_homology_Forward: ttttGACGTCTGAGCTTTATGAAATAAAGACTTTATATAG	This study	N/A
NPW-large_right_homology_Reverse: ttttACCGGTCTCGTAGGTGATATGTGTCATC	This study	N/A
pdm2 promoter fragment (synthesized): coordinates(dm6): chr2L:12,657,539-12,657,982	This study	N/A
Recombinant DNA		
GMR11F02.Gal4 (in pBPGUw vector)	[20]	
pCFD6	[49]	
TVattp-Pax-Cherry	[39]	
Software and algorithms		
Bowtie2	[50]	http://bowtie-bio.sourceforge.net/bowtie2/index.shtml
MACS2	[44]	https://github.com/macs3-project/MACS
Deeptools	[43]	https://deeptools.readthedocs.io/en/develop/
Homer	[45]	http://homer.ucsd.edu/homer/
Picard		https://broadinstitute.github.io/picard/
Samtools	[42]	http://samtools.sourceforge.net/